Recent developments in HgCdTe photovoltaic detectors[+]

J. RUTKOWSKI*

Institute of Applied Physics, Military University of Technology, Warsaw, Poland

This paper presents an overview of fundamental techniques for p–n junction formation in HgCdTe infrared detectors. At the beginning, the classification of photon detectors and general requirements imposed on these detectors are presented. Further considerations are restricted to modern methods of p–n junction formation, so the current state of the art of different types of HgCdTe photodiodes is presented. The comparison of HgCdTe photodiodes with other infrared detectors is finally described.

1. Introduction

Progress in infrared (IR) detectors technology is connected mainly with semiconductor detectors, which are included in the class of photon detectors. In this class of detectors radiation is absorbed within the material by interaction with electrons, bound to lattice or impurity atoms, or with free electrons. New trends in photon IR detector technologies concern HgCdTe photodiodes, Schottky–barrier photoemissive devices, silicon and germanium detectors, InSb photodiodes, and quantum well infrared photodetectors. In the nearest future HgCdTe alloy seems to be unchallenged as the most important material for high performance, fast single element, and small array IR detectors.

This paper describes with fundamental techniques for p–n junction formation in HgCdTe. We will concentrate principally on cooled photodiodes technology. The characteristics of the photodiodes are presented and compared with characteristics of other types of infrared detectors.

2. Relevant HgCdTe properties

HgCdTe is one of the important materials for IR detectors due to a number of uniquely suitable physical, electronic and thermal properties [1–3]. The electrical and optical properties of HgCdTe are determined by the energy gap structure in the vicinity of the Γ–point of the Brillouin zone. This compound is a direct bandgap semiconductor with an energy bandgap that varies from 1.6 eV for pure CdTe to -0.3 eV for pure HgTe. Its adjustable energy gap covers the entire IR region. HgCdTe detector cut–off wevelengths can be selected throughout the 1.6–25 μm range. Its large optical absorption coefficients enable 10–15 μm thick devices to produce internal quantum efficiencies approaching 100%. In many circumstances, intrinsic recombination mechanisms produce long carrier lifetimes and low thermal generation rates, which in turn permit relatively high operating temperatures.

In addition to band structure, HgCdTe has a number of other advantages for IR detectors. The small lattice mismatch between HgTe and CdTe allows relatively high quality epitaxial heterostructures. Common extrinsic impurities can dope HgCdTe either p or n type. Background impurity concentration is typically less than 10^{15} cm^{-3}, allowing adequate control for p–n junctions. For all these advantages, however, it must be remembered that HgCdTe is a defect semiconductor. High concentrations of native point defects, such as mercury vacancies, can occur at modest temperatures and must be controlled.

The material technology has evolved from bulk grown material producing small wafers to relatively large epitaxial wafers grown in reactors with multiple wafer capability. The device requirements can be met by several epitaxial growth techniques at various stages of

---

* corresponding author: J. Rutkowski, Institute of Applied Physics, Military University of Technology, 2 Kaliskiego Str., 01-489 Warsaw, Poland

[+] Presented at the 12th School of Optoelectronics: Photovoltaics – Solar Cells and Infrared Detectors, Kazimierz Dolny, May 22-24, 1997.

technical maturity. The epitaxial growth is being developed to improve the quality, size, yield, and versatility of the detecting material. The epitaxial growth techniques include: liquid phase epitaxy (LPE) [4, 5], metalorganic chemical vapor deposition (MOCVD) [6, 7] and molecular–beam epitaxy (MBE) [8–10].

HgCdTe IR detectors may be made for operation either in the photoconductive or photovoltaic mode. Compared with photoconductors, photodiodes have several advantages. Firstly, the detectivity of photodiodes can be higher than that of photoconductor with a square root factor of two while at the background limited infrared photodetector (BLIP) condition. Secondly, their response time is limited by several transit times, while for the photoconductors, it is related to the lifetime of carriers as well as detectivity.

3. Junction formation

The baseline detector architecture, for all of the cut–off wavelengths required, is a P–on–n double layer planar heterostructure (DLPH) diode. In these photodiodes the base n–type layers are sandwiched between CdZnTe substrate and wider–gap P regions. The second important detector architecture is a n^+–on–p homojunction. In such diodes, the lightly doped narrow gap absorbing region ("base" of the photodiode), determines the dark current and photocurrent. Due to backside illumination (through CdZnTe substrate) and internal electric fields, influence of surface recombinations on the photodiodes performance is eliminated. Proper control of surface passivation, stoichiometric equilibrium, ion implantation, and annealing stages in low–defect high–purity epitaxial layers led to control of high–quality diode technology.

The p–n junction in HgCdTe typically use a deliberate or background donor impurity for the n side of the junction and either vacancy doping or a different acceptor impurity for the p side. The former junction type is the oldest and still forms the diode baseline for several companies in the IR community. Formation a vacancy–doped junction requires a source of Hg atoms, either a vapor over the sample or atoms freed from the lattice itself by damage induced by ion implantation or ion milling.

Hg in–diffusion into HgCdTe with native acceptor concentration of 10^{17} cm^{-3} is perhaps the most widely used for very fast photodiodes, in which a low concentration 10^{14} cm^{-3} n–type region is necessary for large depletion width to reduce junction capacitance.

If implantation is used, the implanted species is typically a donor when activated. It allows to increase donor concentration near the surface and to decrease contact resistance. Boron, indium, aluminium, and mercury have been used as n–type dopants, and phosphorus, arsenic, and copper have been used as p–type dopants. The implanted junctions are formed primarily in p–type material since the implantation process creates an n–type damage region due to the ion–beam bombardment. The junction is formed by Hg interstitials from the implant damage region diffusing into the crystal and annihilating Hg vacancies. Recent results, however, have shown that p–type arsenic implantation can be activated in n–type HgCdTe by thermal annealing under a Hg atmosphere in a high pressure system.

An important development in the evolution of HgCdTe photodiode technology is the capability to grow double layers of controlled composition and doping. This heterostructure technology is employed to grade the bandgap from a narrowband absorber at the substrate to a wide bandgap cap layer at the surface. Currently, three epitaxial growth methods are being intensively investigated for heterojunction technology.

The p–n HgCdTe junctions may be fabricated in any of too configurations: the planar diode and the mesa diode. The choice of a particular structure is based on available processing and materials technology.

3.1. Ion implantation

Ion implantation is one of several alternative techniques for junction formation in HgCdTe photodiodes [11–15]. A summary of the complex phenomena associated with ion implantation in HgCdTe is shown in Fig. 1. In this figure, the typical profile implanted species atom concentrations and corresponding carrier concentrations before and after post–implant anneal are sketched. A fundamental concept developed in the work of light species (B, Be) implantation in HgCdTe is the

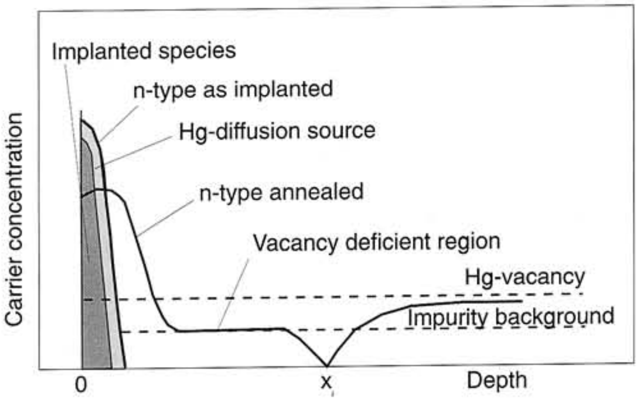

Fig. 1. Phenomena associated with the irradiation process of implantation.

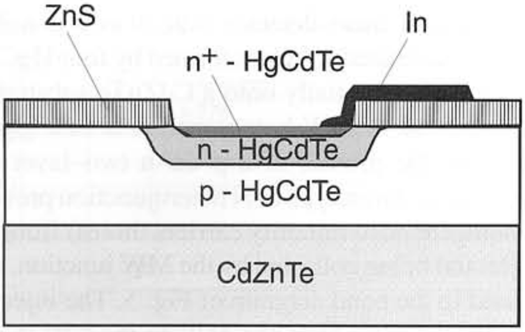

Fig. 2. Cross sectional view of the planar HgCdTe ion implanted photodiode.

generation of free Hg atoms by irradiation process of ion implantation, and their diffusion from the implanted source. This concept is the basis of n–on–p junction formation in certain conditions of background type and concentration of carriers by the diffusion of Hg from the implant–induced Hg source, as illustrated in Fig. 1. When the net background doping is n–type, the annihilated region is n–type. The junctions thus formed are of n^+–n–p type. This is the most desirable case since the junction is located away from the implant–defect region in material which is free of irradiation–induced defects.

A cross sectional view of the photodiode is shown in Fig. 2. The p–n junction was fabricated by ion implantation in a photoresist window of sizes 30 × 30 – 200 × 200 μm^2 with subsequent annealing. The depth of the n–layer is defined by the time and temperature of the annealing process.

3.2. Mesa heterostructure

Current p–on–n HgCdTe LWIR photovoltaic fabrication technology is based on a mesa device configuration [4, 5]. A schematic of mesa heterostructure used in fabrication P^+–n HgCdTe photodiodes is illustrated in Fig. 3. The n–type base, which is the absorbing region, has a thickness 10–20 μm and is deliberately doped with indium at a level of about $(1–3) \times 10^{15}$ cm^{-3}. The composition of the base material is chosen for the wavelength of interest. P–n junction is formed using arsenic as the dopand at a level of about 10^{18} cm^{-3}. To activate As as an acceptor, it must occupy a Te site in the lattice. This requires either growth or annealing at relatively high temperatures under cation–rich conditions. Liquid phase epitaxy growth from a Hg melt satisfies this condition automatically (although some postgrowth annealing may be required). Metalorganic chemical vapor deposition and molecular beam epitaxy have been successfully accomplished in arsenic doping growth. Arsenic has also been diffused from Hg solution and from implants. P–type capping layers with composition $y > x$ has a thickness 1–2 μm. The electrical junction is positioned near the metallurgical interface and it is wise to place the junction in the small band gap layer to avoid deleterious effects on the quantum efficiency and dark currents. Passivation of HgCdTe has been done by several techniques. Recently, however, most laboratories are using CdTe or CdZnTe (deposited by MBE, MOCVD, sputtering and e–beam evaporation) for photodiode passivation.

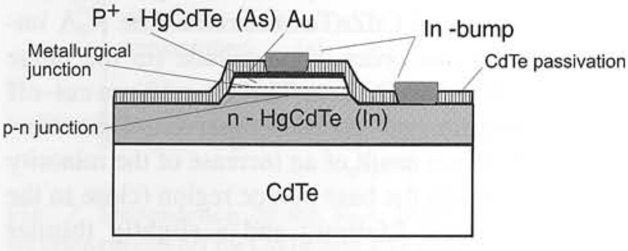

Fig. 3. Schematic of the mesa P^+–n HgCdTe diode heterostructure.

3.3. Planar heterostructure

A critical step in the processing of mesa devices is the etching and deposition of CdTe as a passivant to reduce surface currents. The planar devices were formed using a $Hg_{0.72}Cd_{0.28}Te/Hg_{0.775}Cd_{0.225}Te$ heterostructure grown by molecular beam epitaxy [16, 17]. In Fig. 4 a scheme of the planar HgCdTe diode heterostructure is shown. The formation of planar photodiodes was achieved by first selective implanting of arsenic through a ZnS mask and then diffusing the

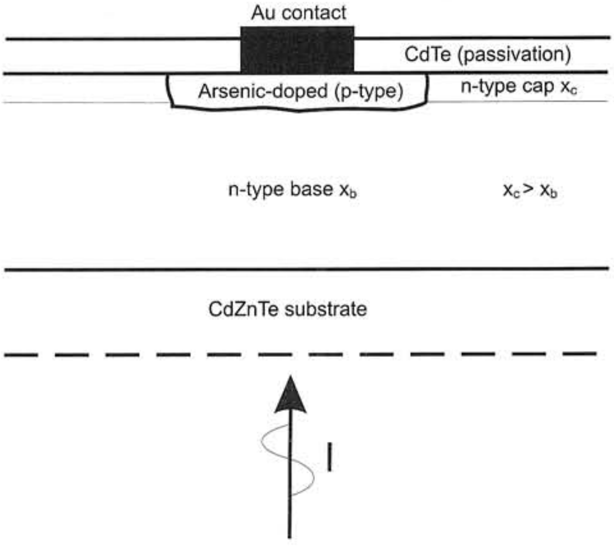

Fig. 4. Schematic drawing of the planar HgCdTe diode heterostructure (after Ref. 16).

arsenic (by annealing at high temperature) through the cap layer into the narrow gap base layer. The selective implantation of arsenic was carried out at room temperature. After the structure was selectively implanted, it was annealed under Hg overpressure in a high pressure system. The first annealing was carried out to diffuse the arsenic into the base LWIR layer and to make the doped region p–type by substitution of arsenic atoms on the Te sublattice, while the second one was carried out to annihilate Hg vacancies formed in the HgCdTe lattice during growth and diffusion of arsenic. Using this technique the planar devices were fabricated of the following areas: 30 × 30 – 500 × 500 μm^2. The planar devices were further protected (as illustrated in Fig. 4.) with polycrystalline CdTe (thickness 1 μm) deposited at room temperature in an e–beam system. Electrical contacts were made with alloyed gold on top of the p–type capping layer and with indium on the n–type layer.

3.4. Dual–band detectors

As the IR technology continues to advance, there is a growing demand for multispectral detectors for advanced IR systems with better target discrimination and identification [18]. One of such two–color HgCdTe detetcor that has been recently reported is the four–layer double heterojunction structure used to produce sequential mode dual–band detectors. Figure 5 shows cross section of these detector [19]. It is a p–n–N–P backside–illuminated structure formed by four HgCdTe layers grown sequentially onto a CdZnTe substrate: a two–layer N–on–P MW homojunction is first grown, followed by the growth of a p–on–n two–layer LW homojunction. An isotype n–N heterojunction prevents LW photogenerated minority carriers (holes) from diffusing to and being collected by the MW junction, as is illustrated in the band diagram of Fig. 5. The injection of minority carriers from the MW to the LW is possible, which could lead to spectral crosstalk in the LW response spectrum, as in the case of the simple bias–selectable device. However, the independent electrical access prevents this from happening by fixing the bias voltage for each junction, so that neither is electrically floating.

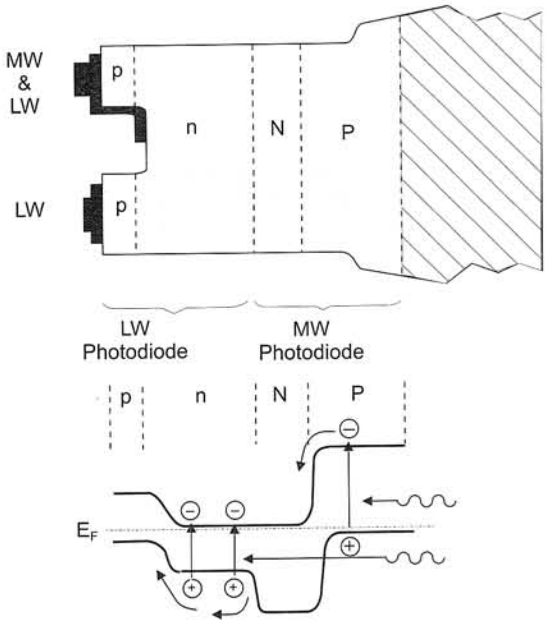

Fig. 5. Cross section and energy band diagram of the independently accessed back–to–back HgCdTe photodiode dual–band detector (after Ref. 19).

The above detectors with two bumps per unit cell for electrical, mechanical, and thermal interconnections can be implemented in large dual–band IR hybrid FPAs. One bump contacts only the p–type region of the LW photodiode; the other bump contacts the n–type region of the LW photodiode, and therefore also the n–type region of the MW photodiode, through an over–the–edge metalization. This way the LW photodiode is accessed directly through the two bumps, while the MW photodiode is accessed through the contact to the n–type region and the array ground.

4. Photodiode characteristics

The most widely used figure of merit to characterize both the dark current and the thermal noise of an infrared photodiode is the R_oA product, defined as the product ot the diode resistance R_o at zero bias voltage and the photodiode active area A. Usually one current mechanism will be dominant over the others, depending on the operating temperature and cut–off wavelength [2].

Destefanis and Chamonal have developed a modified process for planar n^+–p HgCdTe homojunctions with a large improvement in detector performance [14]. The n^+–p homojunctions were made by ion implantation in 8–12 μm thick HgCdTe liquid phase epilayers on CdZnTe substrates. The R_oA improvement of one order of magnitude (in the range between 400 to 650 Ωcm^2 at 77 K for a 10 μm cut–off wavelength detector) has been observed. This effect was obtained as a result of an increase of the minority carrier lifetime in the base p–type region (close to the Auger 7 limited lifetime) and a slightly thinner epitaxial p–type layer. Figure 6 presents the current–voltage (I–V) characteristics of an HgCdTe ion–im-

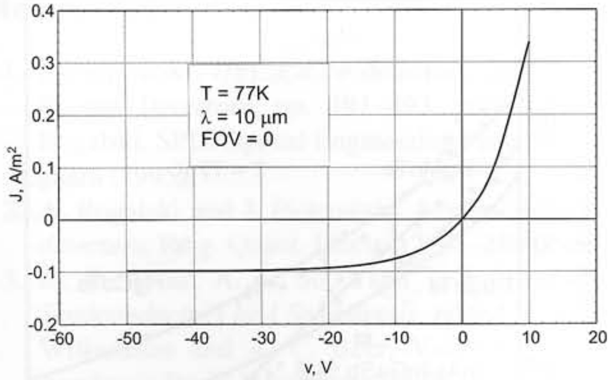

Fig. 6. Current–voltage characteristic of an HgCdTe ion–implanted photodiode (after Ref. 14).

planted photodiode. Under a zero field of view (FOV) at 77 K, the R_oA product of this photodiode, with a cut–off wavelength of 10 μm, is 655 Ωcm^2. The I–V characteristics of heterostructure photodiodes are very similar [4, 5].

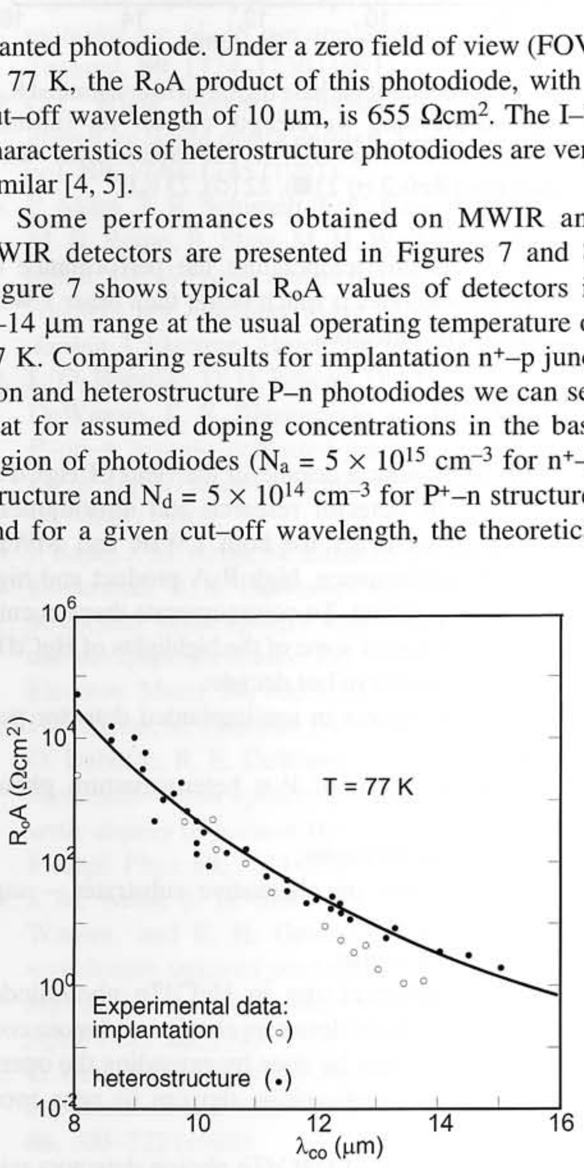

Fig. 7. Dependence of the R_oA product on the long wavelength cut–off for LWIR HgCdTe photodiodes at 77 K. The experimental values are taken from Refs 3, 12,14 (○) and 4, 5 (•).

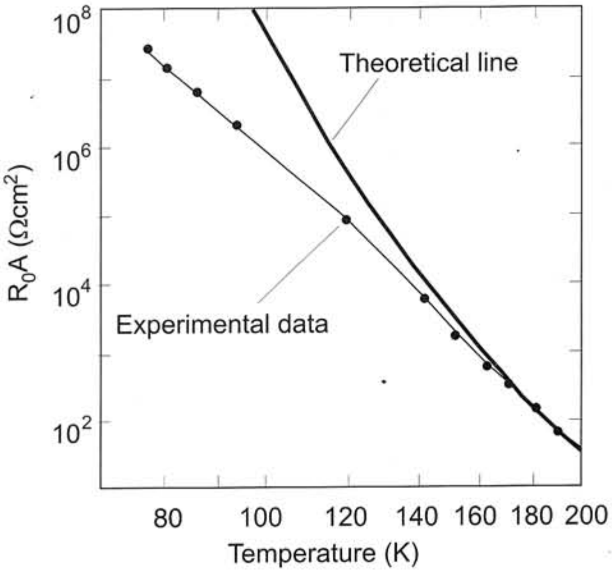

Fig. 8. Dependence of the R_oA product versus temperature for MWIR HgCdTe photodiodes (after Ref. 21).

Some performances obtained on MWIR and LWIR detectors are presented in Figures 7 and 8. Figure 7 shows typical R_oA values of detectors in 8–14 μm range at the usual operating temperature of 77 K. Comparing results for implantation n^+–p junction and heterostructure P–n photodiodes we can see that for assumed doping concentrations in the base region of photodiodes ($N_a = 5 \times 10^{15}$ cm^{-3} for n^+–p structure and $N_d = 5 \times 10^{14}$ cm^{-3} for P^+–n structure) and for a given cut–off wavelength, the theoretical values of R_oA product for P–on–n photodiodes at 77 K are a little greater than for n–on–p photodiodes. The experimental results indicate that the performance of P^+–n heterostructure and n^+–p ion implanted photodiodes exhibit similar R_oA products at 77 K for $\lambda_c < 10$ μm. Conversely, for $\lambda_c > 10$ μm, the R_oA products of n^+–p photodiodes are generally inferior; their quantum efficiency is lower and the impedance is higher. These problems are probably caused by the relative immaturity in fabricating the n–on–p heterostructure, especially in the surface control on the p–side for diodes with a longer wavelength cut–off. However, the earlier calculations above indicate that these differences can be explained by fundamental physical limitation of R_oA products for both types of photodiodes.

Figure 8 shows the variation of this parameter versus temperature for a 5 μm detector at 200 K. The diffusion regime starts at approximately 180 K. At low temperature the performances of the devices are limited by tunnel and surface currents. Sufficiently good agreement of experimental data with expected theoretical values at 200 K is observed. For HgCdTe photodiodes operated at 200 K in 3–5 μm spectral regions the background limited conditions can be easily satisfied.

5. Comparison of HgCdTe photodiodes with other infrared detectors

The detectors operated in the 8–14 μm spectral region include cryogenic photon detectors such as

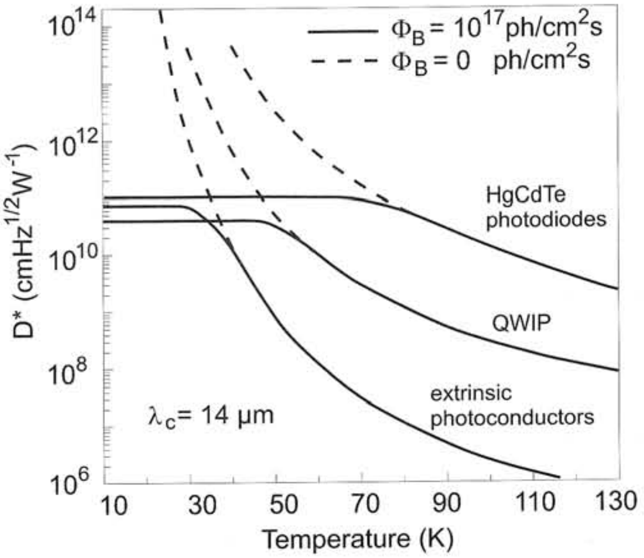

Fig. 9. Theoretical performance limits of LWIR photon and thermal detectors at zero background and background of 10^{17} photons/cm^{2}s, as a function of detector temperature (after Ref. 20).

HgCdTe photodetectors, doped silicon and germanium extrinsic photoconductors, GaAs/AlGaAs quantum well infrared photodetectors (QWIPs) and uncooled thermal detectors (resistive bolometers and pyroelectric detectors) [20]. The temperature dependence of the fundamental limits of D* of these detectors for different levels of background are shown in Fig 9. From Fig. 9 results that in long wavelength IR (LWIR) spectral range, the performance of intrinsic IR detectors (HgCdTe photodiodes) is higher than for other types of photon detectors. HgCdTe photodiodes with background limited performance operate at temperature below ≈ 80 K. HgCdTe is characterised by high optical absorption coefficient and quantum efficiency and relatively low thermal generation rate compared to extrinsic detectors and QWIPs. The extrinsic photon detectors require more cooling than intrinsic photon detectors having the same long wavelength limit. Above relations are modified by influence of background, what is shown in Fig. 9 for a background of 10^{17} photons/cm^{2}s. It is interesting to notice, that the theoretical curves of D* for photon and thermal detectors show similar fundamental limits at low temperatures.

Intrinsic detectors made from new (alternative to HgCdTe) ternary alloy systems such as GaInAs, HgZnTe, HgMnTe, and PbSnTe have been developed recently. The dependence of the base region diffusion limited R$_o$A product on the long wavelength cut–off for intrinsic photovoltaic IR detectors at 77 K is shown in Fig. 10. At this temperature the performance of HgCdTe photodiodes is much better then other LWIR photovoltaic IR detectors.

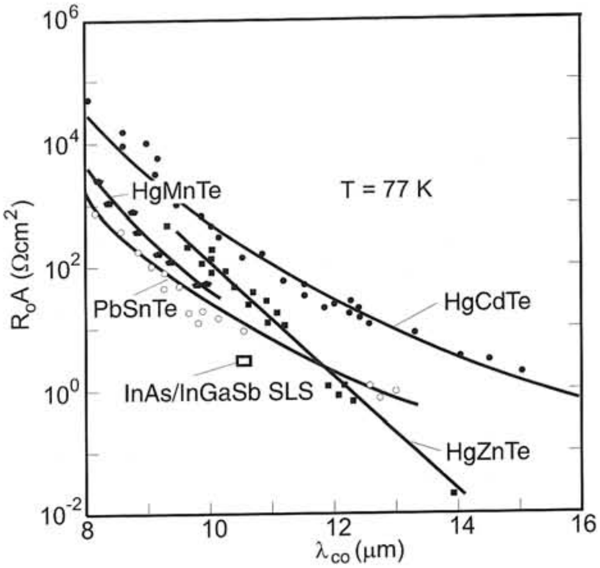

Fig. 10. Dependence of the base region diffusion limited R$_o$A product on the long wavelength cut–off for intrinsic photovoltaic IR detectors at 77 K. The experimental values are taken from Refs 3 (•) 2 (■), 22 (○), 23 (❑).

Conclusion

It has been quite a decade in the field of HgCdTe photovoltaic IR detector research and development. New records were set for both LWIR and MWIR wavelength performance, high R$_o$A product and high temperature operation. To commemorate these events, here is an overview of some of the highlights of HgCdTe photodiode research in last decade:

- large improvement in ion implanted detector performance;
- high performance of P–n heterostructure photodiodes;
- planar heterostructures;
- heterostructures on alternative substrates – sapphire, GaAs, Si;
- dual–band detectors.

Another important aim in HgCdTe photodiodes technology is to make detectors cheaper and more convenient to use. It may be done by extending the operation of HgCdTe photovoltaic devices to near room temperatures.

The comparison of HgCdTe photon detectors with other infrared detectors shows, that HgCdTe photodiodes are the best in LWIR spectral range at 77 K and in MWIR spectral range at 200 K.

References

1. J. Piotrowski, *$Hg_{1-x}Cd_xTe$ detectors*, in *Infrared Photon Detectors*, pp. 391–493, edited by A. Rogalski, SPIE Optical Engineering Press, Bellingham (1995).
2. A. Rogalski and J. Piotrowski, *Intrinsic infrared detectors*, Prog. Quant. Electr. **12**, 87–289 (1988).
3. M. B. Reine, A. K. Sood and T. J. Treadwell, *Semiconductors and Semimetals*, edited by R. K. Willardson and A. C. Beer, Vol. 18, p. 157, Academic Press, New York (1981).
4. G. N. Pultz, P. W. Norton, E. E. Krueger and M. B. Reine, *Growth and characterization of p–on–n HgCdTe liquid–phase epitaxy heterojunction material for 11–18 μm applications*, J. Vac. Sci. Technol. **B9**, 1724–1730 (1991).
5. C. C. Wang, *Mercury cadmium telluride junctions grown by liquid phase epitaxy*, J. Vac. Sci. Technol. **B9**, 1740–1745 (1991).
6. P. Mitra, T. R. Schimert, F. C. Case, S. L. Barnes, M. B. Reine, R. Starr, M. H. Weiler and M. Kestigian, *Metalorganic chemical vapor deposition of HgCdTe p/n junctions using arsenic and iodine doping,* J. Electron. Mater. **24**, 1077–1085 (1995).
7. L. O. Bubulac, D. D. Edwall, D. McConnell, R. E. DeWames, E. R. Blazejewski and E. R. Gertner, *P–on–n arsenic–activated junctions in MOCVD LWIR HgCdTe/GaAs,* Semicon. Sci. Technol. **5**, S45–S48 (1990).
8. J. Bajaj, J. M. Arias, M. Zandian, J. G. Pasko, L. J. Kozlowski, R. E. DeWames and W. E. Tennant, *Molecular beam epitaxy material characteristics and device performance: Reproducibility status,* J. Electron. Mater. **24**, 1067–1076 (1995).
9. J. M. Arias, M. Zandian, J. G. Pasko, S. H. Shin, L. O. Bubulac, R. E. DeWames and W. E. Tennant, *Molecular–beam epitaxy growth and in situ arsenic doping of p–on–n HgCdTe heterojunctions*, J. Appl. Phys. **69**, 2143–2148 (1991).
10. J. M. Arias, S. H. Shin, J. G. Pasko, R. E. DeWames, and E. R. Gertner, *Long and middle wavelength infrared photodiodes fabricated with $Hg_{1-x}Cd_xTe$ grown by molecular beam epitaxy*, J. Appl. Phys. **65**, 1747–1753 (1989).
11. G. Destefanis, *Electrical doping of HgCdTe by ion implantation and heat tretment,* J. Cryst. Growth **86**, 700–722 (1988).
12. L. O. Bubulac, *Defects, diffusion and activation in ion implanted HgCdTe,* J. Cryst. Growth **86**, 723–734 (1988).
13. R. E. DeWames, G. M. Williams, J. G. Pasko and A. H. B. Vanderwyck, *Current generation mechanisms in small band gap HgCdTe p–n junctions fabricated by ion implantation*, J. Crystal Growth **86**, 849–858 (1988).
14. G. Destefanis and F. P. Chamonal, *Large improvement in HgCdTe photovoltaic detector performances at LETI*, J. Electron. Mater. **22**, 1027–1032 (1993).
15. A. Ajisawa and N. Oda, *Improvement in HgCdTe diode characteristics by low temperature post–implantation annealing,* J. Electron. Mater. **24**, 1105–1111 (1995).
16. J. M. Arias, J. G. Pasko, M. Zandian, S. H. Shin, G. M. Williams, L. O. Bubulac, R. E. DeWames, and W. E. Tennant, *Planar p–on–n HgCdTe heterostructure photovoltaic detectors,* Appl. Phys. Lett. **62**, 976–978 (1993).
17. J. M. Arias, J. G. Pasko, M. Zandian, L. J. Kozlowski, and R. E. DeWames, *Molecular beam epitaxy HgCdTe infrared photovoltaic detectors,* Opt. Eng. **33**, 1422–1428 (1994).
18. O. K. Wu, *HgCdTe for cooled and uncooled IRFPAs: Dual–band detectors and beyond*, Compound Semiconductor, 26–27 (July/August 1996).
19. M. B. Reine, P. W. Norton, R. Starr, M. H. Weiler, M. Kestigian, B. L. Musicant, P. Mitra, T. Schimert, F. C. Case, I. B. Bhat, H. Ehsani, and V. Rao, *Independently accessed back–to–back HgCdTe photodiodes: A new dual–band infrared detector,* J. Electron. Mater. **24**, 669–678 (1995).
20. K. Adamiec, A. Rogalski, J. Rutkowski, *Progress in infrared detector technology,* J. Tech. Phys. **38**, 431-488 (1997).
21. L. J. Kozlowski, *HgCdTe focal plane arrays for high performance infrared cameras*, Proc. SPIE **31**, 200–211 (1997).
22. H. Zogg, S. Blunier, T. Hoshino, C. Maissen, J. Masek and A. N. Tiwari, *Infrared sensor arrays with 3–12 μm cutoff wavelengths in heteroepitaxial narrow-gap semiconductors on silicon substrates,* IEEE Trans. Electron Devices **38**, 1110–1117 (1991).
23. J. L. Johnson, L. A. Samoska, A. C. Gossard, J. L. Merz, M. D. Jack, G. H. Chapman, B. A. Baumgratz, K. Kosai and S. M. Johnson, *Electrical and optical properties of infrared photodiodes using the $InAs/Ga_{1-x}In_xSb$,* J. Appl. Phys. **80**, 1116–1127 (1996).